IFIC/11-31

Soft masses in SUSY SO(10) GUTs with low intermediate scales

Valentina De Romeri,* Martin Hirsch,† and Michal Malinský‡
AHEP Group, Instituto de Física Corpuscular – C.S.I.C./Universitat de València
Edificio de Institutos de Paterna, Apartado 22085, E–46071 València, Spain

The specific shape of the squark, slepton and gaugino mass spectra, if measured with sufficient accuracy, can provide invaluable information not only about the dynamics underpinning their origin at some very high scale such as the unification scale $M_{\rm G}$, but also about the intermediate scale physics encountered throughout their RGE evolution down to the energy scale accessible for the LHC. In this work, we study general features of the TeV scale soft SUSY breaking parameters stemming from a generic mSugra configuration within certain classes of SUSY $SO(10)$ GUTs with different intermediate symmetries below $M_{\rm G}$. We show that particular combinations of soft masses show characteristic deviations from the mSugra limit in different models and thus, potentially, allow to distinguish between these, even if the new intermediate scales are outside the energy range probed at accelerators. We also compare our results to those obtained for the three minimal seesaw models with mSugra boundary conditions and discuss the main differences between those and our $SO(10)$ based models.

I. INTRODUCTION

All proposed supersymmetry (SUSY) breaking schemes have to introduce some high energy scale, where soft terms are generated. This scale could be as high as the scale of Grand unification (GUT), or even the Planck scale in gravity mediated schemes [1, 2], or as low as a 100 TeV, for example in gauge mediated SUSY breaking (GMSB) [3]. SUSY particle masses at the electro-weak (TeV) scale then have to be calculated from the fundamental parameters of the models using renormalization group equations (RGEs). Although those fundamental parameters are a priori unknown, at least in minimal schemes there exist certain sum rules for SUSY particle masses, which allow to test the different SUSY-breaking mechanisms, as has been shown for the example of minimal Supergravity (mSugra) already some time ago [4]. Based on the detailed studies of the capabilities of the LHC and ILC experiments to measure SUSY particle masses [5–7], the accuracy with which different SUSY-breaking schemes can be tested has since then been calculated by a number of authors, for a few examples see [8–12].

However, most of these studies concentrated on models in which the particle spectrum between the electroweak and the SUSY-breaking scale was exactly that of the Minimal Supersymmetric extension of the Standard Model (MSSM). Evolution under RGEs is, however, sensitive to the particle content of the theory. Thus, in principle, any superfield beyond the MSSM (with mass below the SUSY-breaking scale) will leave its imprint on the soft parameters. The specific shape of the squark, slepton and gaugino mass spectra, if measured with sufficient precision, can therefore provide invaluable information not only about the dynamics underpinning their origin, but also about physics at intermediate scales. In this paper, we study soft SUSY-breaking masses within certain classes of SUSY $SO(10)$ theories with different intermediate symmetries below the GUT scale $M_{\rm G}$. Our main motivation to study these models comes from the observed neutrino masses [13–15] and the possibility that supersymmetry might be discovered soon at the LHC.

In the MSSM, if SUSY particles have TeV-scale masses[1], the gauge couplings unify (nearly) perfectly at around $M_{\rm G} \sim 2\times10^{16}$ GeV. Adding new particles beyond the MSSM spectrum can easily spoil this attractive feature and, thus, the requirement of gauge coupling unification (GCU) imposes a severe constraint on SUSY model building. However, neutrino oscillation experiments [13–15, 18] have shown that at least two neutrino masses are non-zero [19, 20] and at least one neutrino must have a mass $m_{\rm Atm} \geq 0.05$ eV. If neutrinos are Majorana par-

*Electronic address: deromeri@ific.uv.es
†Electronic address: mahirsch@ific.uv.es
‡Electronic address: malinsky@ific.uv.es

[1] Strictly speaking, within SUSY unification requires only gauginos to be light [16, 17], but not necessarily sfermions. We will not entertain this possibility.

ticles, this value indicates that the scale of lepton number violation (LNV), $\Lambda_{\rm LNV}$, can not be larger (but could potentially be much smaller, see below) than roughly $\Lambda_{\rm LNV} \sim 10^{15}$ GeV. This value is significantly below $M_{\rm G}$.

In the minimal SUSY $SU(5)$ model neutrinos are massless, just as in the MSSM and for the same reasons. However, it is fairly straightforward to extend minimal $SU(5)$ to include a seesaw mechanism which allows to explain the observed smallness of the neutrino masses. It is well known that, at the renormalizable level, there are exactly three ways [21] to do so: (i) Add (at least two) gauge singlet superfields, i.e. "right-handed neutrinos", this is now usually called type-I seesaw [22–24]; (ii) add a scalar triplet with $Y = 2$ (type-II seesaw) [25, 26]; or (iii) add (two or more) *fermionic* triplets with $Y = 0$ (type-III seesaw) [27]. For the latter two cases, the successful unification of the MSSM can only be maintained if these heavy fields enter in complete $SU(5)$ multiplets. Thus, within SUSY models, GCU requires the type-II seesaw to be realized by adding a pair of Higgs 15-plets, while a type-III seesaw can be generated with (at least two) copies of 24-plets in the matter sector [21].

If we require Yukawas to be perturbative anywhere between the seesaw scale (i.e., $\Lambda_{\rm LNV}$) and the GUT scale $M_{\rm G}$, all three types of seesaw require $\Lambda_{\rm LNV}$ to be below 10^{15} GeV. If we ask in addition that all gauge couplings remain perturbative, lower limits on SUSY type-II seesaw of the order of $\Lambda_{\rm LNV} \gtrsim 10^7$ GeV at 1-loop (or $\Lambda_{\rm LNV} \gtrsim 10^9$ GeV at 2-loop) [28] result. For type-III seesaw, perturbativity puts lower bounds on the seesaw scale of the order of $\Lambda_{\rm LNV} \gtrsim 10^{13}$ GeV for three copies of **24** of $SU(5)$ and around $\Lambda_{\rm LNV} \gtrsim 10^9$ GeV for two[2] copies of **24**. Since type-I seesaw adds only Standard Model (SM) singlets, there is no *lower* limit on its scale from perturbativity.

Models based on $SO(10)$ [30] are different from $SU(5)$ in that they automatically contain the necessary ingredients to generate non-zero neutrino masses: (i) The spinorial **16** of $SO(10)$ contains a complete SM family plus a gauge singlet, i.e. a right-handed neutrino. In addition, (ii) $U(1)_{B-L}$ is a subgroup of $SO(10)$. If the $U(1)_{B-L}$ is broken by $SU(2)_R$ triplets with $B - L = 2$, a seesaw mechanism of either type-I and/or type-II results automatically [24]. Alternatively, breaking $U(1)_{B-L}$ by $SU(2)_R$ doublets can give different realizations of the so-called inverse [31] and linear [32] seesaw schemes.

The $SO(10)$ gauge symmetry can be broken to the SM gauge group in a variety of ways [33]. Since our main motivation is neutrino masses, all breaking chains of interest to us contain a left-right symmetry (LR) at some stage. SUSY LR models which use triplets to break $SU(2)_R$, whether using only $B - L = 2$ triplets [34, 35] or both $B - L = 2$ and $B - L = 0$ triplets [36, 37], all require that the scale of $SU(2)_R$ breaking (v_R) is close to the GUT scale, typically $v_R \geq 10^{15}$ GeV from GCU. However, also in non-minimal versions of triplet-based models, one can not lower v_R arbitrarily, since one encounters either problems with proton decay or with perturbativity [38]. Allowing for either (a) sizeable GUT scale threshold corrections, (b) non-renormalizable operators or (c) adding some carefully chosen particles the authors of [39] find a lower limit on v_R of the order of $v_R \sim 10^9$ GeV.

However, the situation is different in models with doublets. It was shown in [40] that if one breaks $SU(2)_R \times U(1)_{B-L}$ by means of an $B - L = 0$ triplet to $U(1)_R \times U(1)_{B-L}$ and, subsequently, the $U(1)_R \times U(1)_{B-L}$ symmetry gets broken down to $U(1)_Y$ by the Y-neutral components of $SU(2)_R$ doublets, it is possible to construct models in which the scale of $U(1)_R \times U(1)_{B-L}$ breaking, v_{BL}, can be as low as TeV. In [39] it was demonstrated that even the full $SU(2)_R$ can be brought down to the electro-weak scale, if only doublets are used in the symmetry breaking and if some additional particles are also light. An especially simple variant for a low v_R scale was discussed in [41]. Here, GCU is maintained for a TeV scale $SU(2)_R$ with only two requirements: (a) The numbers of light left and right doublets have to be different and (b) a (pair of) light coloured $SU(2)_L$ singlets needs to be added to the spectrum.

Obviously, all models with additional gauge groups lead to a potentially very rich phenomenology at the LHC. Current limits on new Z' (and W_R) gauge bosons are very roughly of the order of $m_{Z'} \gtrsim (5-6)/g$ TeV ($m_{W_R} \gtrsim 1$ TeV) [42, 43], with exact numbers depending on the couplings, so there is ample room for discovery. One expects that for $\sqrt{s} = 14$ TeV at the LHC limits for Z' bosons will improve to at least 3 TeV [44]. A W_R should be discovered at the LHC up to masses of the order of $4 - 4.6$ TeV [45, 46], depending on luminosity. However, even if the new gauge bosons predicted in the models [39–41] are out of reach for the LHC, sparticle mass spectra will contain indirect hints for these new

[2] With only one copy of **24**, the seesaw scale could be lowered as far as the electro-weak scale. However, with only one **24**, neutrino data can not be explained unless non-renormalizable operators are added to the model [29].

scales due to changes in the RGEs, as discussed above. This observations is in fact the main motivation for the calculations presented in this paper.

Within the mSugra framework, one can define certain combinations of soft parameters, which are independent of the high scale input parameters at leading order. We will call such combinations "RGE invariants". In [47] it was pointed out that these invariants show a characteristic deviation from their mSugra expectations, if either a type-II or a type-III seesaw mediators are added to the MSSM spectrum. Here, we will study these invariants in different $SO(10)$ based models. We will construct variants of the models proposed in [40, 41] and will also consider a completely new model, in which v_R can be brought down to the electro-weak scale with the help of an intermediate Pati-Salam scale [48]. We will show how the RGE invariants calculated within these models depart from their mSugra values, how they differ from model to model and, importantly, also differ from the expectations for the minimal type-II and type-III seesaws. The invariants are therefore good indicators to distinguish between different GUT-based SUSY models.

Two comments might be in order at this point. First, our calculations rely on the assumption of strict mSugra boundary conditions. In principle, invariants can be calculated also in more complicated SUSY-breaking schemes, if the SUSY-breaking scale is larger than the mass scale of the new states. However, with a total of only four invariants (per generation) only SUSY-breaking schemes with very few additional parameters will lead to non-trivial consistency tests. Furthermore, while the invariants are certainly useful model discriminators, it has been shown that quantitatively important 2-loop corrections exist for both, the type-II [49] and the type-III seesaw [28]. A quantitative determination of the new intermediate scales will therefore most likely rely on a detailed numerical χ^2-analysis of measured SUSY spectra [50], using invariants only as guidance for which models might be interesting for further scrutiny.

The rest of the paper is organized as follows. In the next section, we shall specify four basic $SO(10)$ models of interest paying particular attention to their potential compatibility with the SM flavour structure. In section III, we briefly comment on the evolution of the soft masses in mSugra models and, for completeness, recall the definitions of the RGE invariants, following essentially the discussion in [49]. The results of a simple analysis of their sensitivity to the intermediate scales in the four scenarios considered here are given in Section IV. Finally we close with a short discussion and outlook. Some technical details of the RGEs in models with more than a single abelian gauge factors are deferred to an Appendix.

II. SPECIFIC SUSY SO(10) GUT MODELS

Let us begin with a detailed specification of the four basic SUSY $SO(10)$ GUTs which shall be the studied in Sect. IV. Though all of them, by construction, accommodate the low-energy measured values of the gauge couplings, they will in general yield vastly different MSSM soft spectra whose shapes would strongly depend on the character of the intermediate symmetries and the scales of their spontaneous breakdown.

A. General remarks

In all cases, we demand that the models should be realistic in several basic aspects and potentially interesting for our scope, namely:

- Requirement 1: SUSY $SO(10)$ unification with a sliding intermediate scale by which we mean that the position of a certain intermediate scale can be moved over a large energy range whilst the full compatibility with the electroweak constraints is maintained. This is a basic practical stipulation in order to be able to study the scale-dependence of the soft leading-log RGE invariants in such GUTs over a large range.

- Requirement 2: Renormalizable $SO(10) \to$ MSSM gauge symmetry breaking - this is namely to have a good grip on the intermediate scales and the associated thresholds.

- Requirement 3: Potentially realistic fermionic spectra - we demand that the effective Yukawa structure is rich enough to be able, at least in principle, to accommodate the low-energy matter-fermionic spectra and mixing. The sliding nature of the $SU(2)_R \times U(1)_{B-L}$ scale, however, typically calls for a non-canonical seesaw, such as inverse [31] or linear [32] seesaw.

- Requirement 4: MSSM Higgs doublet structure suitable for the implementation of the standard radiative symmetry breaking and also as a means

to get unrelated Yukawa couplings for quarks and charged leptons.

As to the Requirement 1 above, we shall be namely interested in SUSY $SO(10)$ models with a sliding $SU(2)_R$ breaking scale which would be assumed to range from as low as several TeV up to essentially the GUT scale. From the gauge unification perspective, there are two basic strategies to devise such Models. In practice:

- One can attempt to compensate for the departure of the b-coefficients from their "canonical" MSSM values (due to the presence of $W_R^\pm$ and the $SU(2)_R$-breaking Higgs multiplets in the desert) by other multiplets brought down to the $SU(2)_R$-breaking scale, which would inflict further shifts to the b-coefficients (namely g_3) in order to compensate for the genuine low-scale $SU(2)_R$ effects. The main advantage of this approach is that $SU(2)_R \times U(1)_{B-L}$ becomes the only intermediate scale at play, so the $SO(10)$ gauge symmetry is broken down to the $SU(3)_c \times SU(2)_L \times U(1)_Y$ of the MSSM in just two steps. The slight complication here is the fact that the gauge-coupling unification in such a case is not exact, which brings an extra theoretical uncertainty into the game. [3]

- Alternatively, rather than compensating for the departure of the b-coefficients from their MSSM values due to the $W_R^\pm$ (and the associated Higgs multiplets) in the desert, one can take advantage of this and invoke an extra intermediate scale such as for instance $SU(4)_C \times SU(2)_L \times SU(2)_R$ of Pati and Salam and let it conspire with the $SU(2)_R \times U(1)_{B-L}$ so that the gauge unification is maintained. Though this can be somewhat more elaborate in practice, the clear advantage of such a scenario is that one can always devise an exact gauge coupling unification by a proper adjustment of the Pati-Salam scale.

In both cases, because we have quite a lot of beyond-MSSM dynamics in the desert, we expect significant effects of the relevant intermediate scale(s) on the shape of the MSSM squark and slepton spectra.

The first strategy above, especially in combination with the other requirements, is rather restrictive. Indeed, it imposes strict conditions on the b-coefficients in specific models which should essentially match those of the MSSM up to a uniform shift. Nevertheless, a variety of potentially realistic models can still be devised and, in particular, the behaviour of the RGE invariants in this class of theories can be strongly model-specific. We shall demonstrate this on a couple of scenarios of this kind derived from [41], c.f., Model I and Model II in section II B.

The sensitivity to the intermediate-scales dynamics should be even more pronounced in the latter class of scenarios with more than a single such scale at play. This is namely due to the fact that the extra fields in the desert associated to a higher intermediate symmetry (e.g., Pati-Salam) tend to affect the soft spectra stronger than in the former case with an intermediate $SU(3)_c \times SU(2)_L \times SU(2)_R \times U(1)_R$ only. This feature is going to be clearly visible in the specific model of this kind, c.f., Model III in section II B.

However, a strong dependence of the invariants on the sliding scale should not be viewed as a generic feature of the SUSY $SO(10)$ GUTs. Indeed, there are simple scenarios in which the sliding intermediate scale does leave almost no imprints in the soft spectrum. We shall demonstrate this on a specific model with a sliding intermediate $U(1)_{B-L}$ scale (and a fixed $SU(2)_R$ scale at around 10^{14} GeV ensuring a proper gauge unification) of the kind given in [40], c.f., Model IV in the section II B. Here, the GUT-scale pattern of the RGE invariants is (almost) not changed by the running, leaving no good handle on the intermediate scale in the SUSY spectrum.

B. SUSY $SO(10)$ models with a sliding $SU(2)_R$ scale

1. *Models I and II: single sliding intermediate scale*

First, we shall introduce two variants of the model advocated in [41] which supply the original setting with a few extra ingredients in order to make it potentially realistic, c.f., Sect. II A.

a. Model I: The field content relevant to the running in this Model is specified in TABLE I.

The original $SO(10)$ gauge symmetry is broken down to the MSSM in two steps via an intermediate $SU(3)_c \times SU(2)_L \times SU(2)_R \times U(1)_{B-L}$ symmetry stage. The first step, i.e., the $SO(10) \to SU(3)_c \times SU(2)_L \times SU(2)_R \times U(1)_{B-L}$ breaking, is triggered by an interplay between the VEVs of 45 and 210 of $SO(10)$. Subsequently, the

[3] This feature is already present at the MSSM level.

Field	Multiplicity	$3_c 2_L 2_R 1_{B-L}$	$SO(10)$ origin
Q	3	$(3,2,1,+\frac{1}{3})$	16
Q^c	3	$(\bar{3},1,2,-\frac{1}{3})$	16
L	3	$(1,2,1,-1)$	16
L^c	3	$(1,1,2,+1)$	16
S	3	$(1,1,1,0)$	1
δ_d, $\bar{\delta}_d$	1	$(3,1,1,-\frac{2}{3})$, $(\bar{3},1,1,+\frac{2}{3})$	10
Φ	1	$(1,2,2,0)$	10, 120
χ, $\overline{\chi}$	1	$(1,2,1,\pm 1)$	$\overline{16}$, 16
χ^c, $\overline{\chi}^c$	3	$(1,1,2,\mp 1)$	$\overline{16}$, 16

TABLE I: The relevant part of the field content of Model I with a sliding $SU(2)_R$-breaking scale discussed in section II B 1 a. In the third column the relevant fields are characterized by their $SU(3)_c \times SU(2)_L \times SU(2)_R \times U(1)_{B-L}$ quantum numbers while their $SO(10)$ origin is specified in the fourth column.

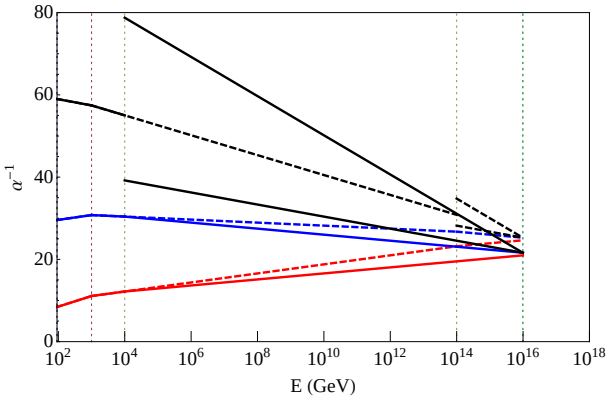

FIG. 1: Gauge coupling unification in Model I in two limits corresponding to different positions of the sliding $SU(2)_R \times U(1)_{B-L}$ breaking scale V_R. In solid lines, we depict the RGE behaviour of the gauge couplings for V_R in the vicinity of the electroweak scale $V_R \sim 10^4$GeV while the dashed lines correspond to $V_R \sim 10^{14}$GeV. The position of the intersection region shifts slightly up with rising V_R but the corresponding scale remains intact.

$SU(2)_R \times U(1)_{B-L}$ gauge symmetry is broken down to the $U(1)_Y$ of hypercharge by the VEVs of the $\chi^c \oplus \overline{\chi}^c$ pair which can emerge for instance from its cubic interaction with a full singlet ρ[4]. Note that, at the one-loop level, such a neutral ρ field can be put essentially anywhere between M_{GUT} and M_{SUSY} without any impact on the gauge unification. The b_i-coefficients at the $SU(3)_c \times SU(2)_L \times SU(2)_R \times U(1)_{B-L}$ level read $b_3 = -2$, $b_L = 2$, $b_R = 4$ and $b^c_{B-L} = 13$ where the last number corresponds to the canonically normalized $B-L$ charge, which is obtained from the "physical" one (based on $B^p_Q = +\frac{1}{3}$ and $L^p_L = +1$) by means of the formula $(B-L)^c = \sqrt{\frac{3}{8}}\,(B-L)^p$. Note that these coefficients happen to be entirely identical to the setting advocated in [41] and, thus, the leading-log evolution of the soft SUSY-breaking parameters in that Model is covered by our analysis of Model I, see Sect. IV A. The scale of the $SU(2)_R \times U(1)_{B-L}$ breaking is not determined because it drops from the formula for the unification scale (owing namely to the hypercharge-matching condition $\alpha_Y^{-1} = \frac{3}{5}\alpha_R^{-1} + \frac{2}{5}\alpha_{B-L}^{-1}$) and affects only the value of the GUT-scale gauge coupling α_G which, however, is subject of much weaker constraints.

This, on one hand, makes the gauge coupling unification in Model I qualitatively similar to the MSSM case, see FIG. 1. On the other hand, it is well known that in the MSSM the one-loop gauge unification is incompatible with the latest extractions of α_s unless the soft SUSY-breaking scale is pushed well below 1 TeV. This few percent mismatch is expected to be accounted for by GUT-scale thresholds whose detailed analysis is, however, beyond the scope of this work. Thus, in what follows, we shall simply parametrize our ignorance of the shape of the GUT spectrum by considering unification regions from where the $SU(3)_c \times SU(2)_L \times SU(2)_R \times U(1)_{B-L}$ gauge couplings can emanate rather than unique unification points, c.f., FIG. 5 and discussion in Sect. IV A. Though this approach is oversimplified in several aspects, it admits to estimate the magnitude of the theoretical error associated to the lack of exact gauge-coupling unification in this model.

Concerning the effective flavour structure of the model, there are two aspects worth some discussion here, namely, the structure of the effective MSSM Higgs doublet pair Φ and the possibility to accommodate the SM quark and lepton masses and mixing (requirements 3 and 4 formulated at the beginning of this Section). First, the effective L-R bidoublet $(1,2,2,0)$ corresponds to a massless combination of the $(1,2,2)$ and $(15,2,2)$ Pati-Salam components of 10 and 120 of $SO(10)$, respectively, which can mix at the GUT-level due to the PS-breaking VEV in an $SO(10)$-breaking multiplet such as 45 and/or 210. Usu-

[4] It is perhaps worth mentioning that, for a very low scale of the $SU(2)_R \times U(1)_{B-L}$ breaking, the relevant VEV can be devised even without an extra singlet because, then, the interplay between a "RH μ-term" for $\chi^c \oplus \overline{\chi}^c$ and the relevant soft mass should be sufficient, in complete analogy with the $SU(2)_L$-doublet sector in the MSSM.

Field	Multiplicity	$3_c 2_L 2_R 1_{B-L}$	$SO(10)$ origin
Q	3	$(3,2,1,+\frac{1}{3})$	16
Q^c	3	$(\bar{3},1,2,-\frac{1}{3})$	16
L	3	$(1,2,1,-1)$	16
L^c	3	$(1,1,2,+1)$	16
S	3	$(1,1,1,0)$	1
δ_u, $\bar{\delta}_u$	1	$(3,1,1,+\frac{4}{3})$, $(\bar{3},1,1,-\frac{4}{3})$	45
Φ	1	$(1,2,2,0)$	10, 120
χ, $\overline{\chi}$	1	$(1,2,1,\pm 1)$	$\overline{16}$, 16
χ^c, $\overline{\chi}^c$	2	$(1,1,2,\mp 1)$	$\overline{16}$, 16

TABLE II: The same as in TABLE I for Model II defined in Sect. II B 1 b. The main variation with respect to Model I is the $B-L$ charge of the vector-like colour triplet pair owing to its different $SO(10)$ origin. The extra δ_u and $\overline{\delta}_u$ fields can mix with the up-type quarks at the MSSM level which leads to a potentially realistic effective flavour structure. In order to maintain the MSSM-like unification pattern, the number of the $SU(2)_R$ doublets has been reduced, thus making the setting slightly more compact than in Model I.

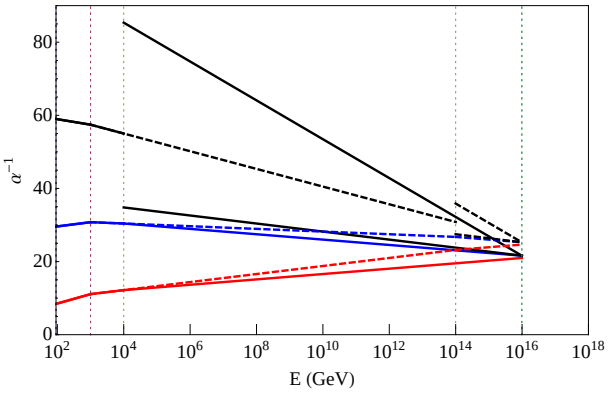

FIG. 2: Gauge coupling unification in Model II in two limits corresponding to different positions of the sliding $SU(2)_R \times U(1)_{B-L}$ breaking scale V_R. In solid lines, we depict the RGE behaviour of the gauge couplings for V_R in the vicinity of the electroweak scale $V_R \sim 10^4$GeV while the dashed lines correspond to $V_R \sim 10^{14}$GeV. The position of the intersection region shifts slightly up with rising V_R but the corresponding scale remains intact.

ally, the role of the extra Higgs such as 120 and/or 126 in the Yukawa sector is namely to provide Clebsch-Gordan coefficients that would break the degeneracy of the effective Yukawa couplings among up and down quarks and charged leptons. However, an extra 120 alone is still not enough as it does not yield enough freedom to accommodate the SM data [55]. Actually, the issue becomes even worse if the MSSM-level mass matrices for the two hypercharge components of Φ are virtually identical, as one can expect for a single bidoublet at play in the low-scale $SU(2)_R$-breaking regime. Both issues are potentially resolved due to the extra vector-like down-type quark pair $\delta_d \oplus \delta_d$ and an additional $SU(2)_L$-doublet Higgs pair $\chi \oplus \overline{\chi}$ (which, simultaneously, ensure the right b-coefficients for the running), c.f., TABLE I. In this case, the down-type quark mass matrix is extended[5] to 4×4 which, together with the extra freedom in the MSSM doublet sector, should be enough to avoid the Grimus-Kuhbock-Lavoura (GKL) no-go [55]. Let us also mention that the VEV of χ_L gives rise to the LS entry in the neutrino mass matrix generating the linear seesaw mechanism and, unlike in [40], it is not naturally suppressed in this case because $\chi \oplus \overline{\chi}$ resides well below the GUT scale. Thus, one has to assume a small $LS\chi$ Yukawa coupling.

[5] For an explicit $SO(10)$ realisation of this mechanism see e.g. [56] and references therein.

b. Model II: The relevant b_i-coefficients at the $SU(3)_c \times SU(2)_L \times SU(2)_R \times U(1)_{B-L}$ level read $b_3 = -2$, $b_L = 2$, $b_R = 3$ and $b^{\rm can}_{B-L} = 29/2$. Indeed, these numbers differ from Model I only in the $SU(2)_R \times U(1)_{B-L}$ sector and the variations in the relevant b-coefficients obey $\Delta b_R + \frac{2}{3}\Delta b_{B-L} = 0$ so the b-coefficient associated to the "effective" MSSM hypercharge is the same as in Model I. Therefore, apart from the difference in the specific slopes of the $SU(2)_R \times U(1)_{B-L}$ curves the qualitative picture of the gauge coupling unification in Model II, c.f. FIG. 2, is very similar to that observed in Model I. Nevertheless, as we shall see in Sect. IV A, even such a slight change in the gauge-coupling behaviour at the $SU(3)_c \times SU(2)_L \times SU(2)_R \times U(1)_{B-L}$ level is enough to generate a significant difference between the Model-I and Model-II soft invariants, especially if the $SU(3)_c \times SU(2)_L \times SU(2)_R \times U(1)_{B-L}$ running is long. However, if the $SU(2)_R \times U(1)_{B-L}$ gauge symmetry happens to be broken close to the GUT scale, the two models will be indistinguishable from the soft-sector point of view.

Concerning the flavour structure of Model II, it is indeed very similar to that of Model I, with the main difference that here the GKL no-go [55] is overcome by a 4×4 extension of the up-type quark mass matrix. Moreover, since it is the VEV of $\overline{\chi}$ rather than that of χ that enters the extended up-type quark mass matrix, $\langle \chi \rangle$ can be made much smaller than $\langle \overline{\chi} \rangle$ which also relieves the need for the small $LS\chi$ Yukawa in the neutrino sector.

Field	Mult.	$3_c 2_L 2_R 1_{B-L}$	Pati-Salam	$SO(10)$
Q	3	$(3,2,1,+\frac{1}{3})$	$(4,2,1)$	16
Q^c	3	$(\bar{3},1,2,-\frac{1}{3})$	$(\bar{4},1,2)$	16
L	3	$(1,2,1,-1)$	$(4,2,1)$	16
L^c	3	$(1,1,2,+1)$	$(\bar{4},1,2)$	16
Σ^c	3	$(1,1,3,0)$	$(1,1,3)$	45
δ_d, $\bar{\delta}_d$	1	$(3,1,1,\mp\frac{2}{3})$	$(6,1,1)$	10
Φ	2	$(1,2,2,0)$	$(1,2,2)$	10
Ω	1	$(1,1,3,0)$	$(1,1,3)$	45
χ, $\overline{\chi}$	1	$(1,2,1,\pm 1)$	$(\bar{4},2,1)$,$(4,2,1)$	$\overline{16}$, 16
χ^c, $\overline{\chi}^c$	1	$(1,1,2,\mp 1)$	$(4,1,2)$,$(\bar{4},1,2)$	$\overline{16}$, 16
Ψ	1	absent	$(15,1,1)$	45

TABLE III: The effective field contents of Model III in the two intermediate symmetry stages.

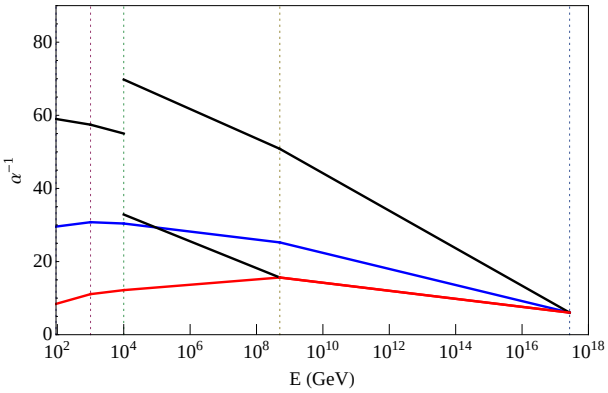

FIG. 3: Running in the Model III variant of the low-LR scale SUSY SO(10). Here the SO(10) gauge symmetry is broken first into a Pati-Salam intermediate stage stretching from the unification point down to the relevant energy scale V_{PS} (in the middle) and, subsequently, to the L-R symmetry stage. The value of V_{PS} is correlated to the position of the L-R breaking scale V_R which can again slide from as low as few TeV up to roughly 10^{14}GeV, c.f., FIG. 8.

Given also the reduced number of the $SU(2)_R$ doublets, Model II constitutes a somewhat more compact alternative to Model I.

2. *Model III: sliding $SU(2)_R$ and Pati-Salam scales*

The third model of our interest belongs to the second category of the simple classification given in Sect. II A. In particular, the sliding nature of the $SU(2)_R \times U(1)_{B-L}$ scale is achieved via an interplay with another intermediate scale, namely, the Pati-Salam $SU(4)_C \times SU(2)_L \times SU(2)_R$, rather than a delicate adjustment à la Model I or Model II owing to very specific field contents. Thus, the initial $SO(10)$ gauge symmetry is broken down to the MSSM in three steps. The field content relevant to the two intermediate-symmetry stages is given in TABLE III. In more detail, the initial $SO(10) \to SU(4)_C \times SU(2)_L \times SU(2)_R$ breaking is triggered by the GUT-scale VEV of 54 of $SO(10)$. The subsequent $SU(4)_C \times SU(2)_L \times SU(2)_R \to SU(3)_c \times SU(2)_L \times SU(2)_R \times U(1)_{B-L}$ breaking is due to the VEV of the Ψ emerging again from its interplay with an extra singlet. Finally, the $SU(2)_R \times U(1)_{B-L}$ symmetry is broken down to the MSSM by means of the VEVs of $\chi^c \oplus \overline{\chi}^c$ which are connected by the $B-L$-neutral $SU(2)_R$-triplet Ω. At the Pati-Salam stage, the b_i-coefficients read $b_4 = 3$, $b_L = 6$, $b_R = 14$ while at the $SU(3)_c \times SU(2)_L \times SU(2)_R \times U(1)_{B-L}$ level they are $b_3 = -2$, $b_L = 3$, $b_R = 11$ and $b^{\rm can}_{B-L} = 10$.

In this model, both the position of the GUT scale as well as the value of α_G depend on both intermediate scales. However, unlike in Models I and II, here the gauge unification can always be made exact, c.f., FIG. 3, even at the one-loop level, and, thus, there is no extra theoretical uncertainty other than the error in the electroweak-scale α_s to be taken into account.

The flavour structure of this model relies on the presence of three extra copies of $SU(2)_R$ triplet Σ^c which in the neutrino sector play a role similar to that of S in Models I and II. In particular, they expand the 6×6 neutrino mass matrix to 9×9 where, e.g., the $L^c\Sigma^c$ sector comes from the contraction with the VEV of χ^c, but without any entry generated at the $L\Sigma^c$ "linear seesaw" position. Thus, there is no need for an extra fine-tuning in the seesaw formula in Model III. Moreover, the charged components of Σ^c can mix with the charged leptons and, hence, provide the welcome departure from the down-type quarks even if the MSSM doublets span over 10's of $SO(10)$ only. Indeed, the relevant 6×6 charged-lepton mass matrix looks schematically like

$$M_\ell \propto \begin{pmatrix} Y v_d^{10} & 0 \\ \langle \overline{\chi}^c \rangle & \mu_{\Sigma^c} + \langle \Omega \rangle \end{pmatrix}, \qquad (1)$$

where the row and column bases are $\{L, \Sigma^{c-}\}$ and $\{L^c, \Sigma^{c+}\}$, respectively, and μ_{Σ^c} is the associated singlet mass parameter. Note also that the VEV of Ω is antisymmetric in the generation space and, thus, does not contribute to the neutrino Majorana mass matrix. Finally, the two MSSM Higgs doublets are different because the underlying bi-doublets contract through Ω and, therefore, the effective up-type quark Yukawa coupling differs from the down-type one even without the need to

resort to the mixing with the vector-like $\delta_d \oplus \bar{\delta}_d$ pair.

C. SUSY $SO(10)$ models with a sliding $U(1)_R$ scale

All the models discussed so far featured an intermediate $SU(2)_R \times U(1)_{B-L}$ symmetry which, at a certain scale, was broken directly down to the $U(1)_Y$ of the MSSM hypercharge. The full $SU(2)_R$, however, is not the minimal option to realize a gauge symmetry acting in the RH sector of the matter spectrum in a way compatible with the MSSM quantum numbers. Indeed, the hypercharge sum-rule $Y = T_R^3 + (B-L)/2$ trivially holds even if one sticks to the $U(1)_R$ subgroup of the original $SU(2)_R$ generated by T_R^3 alone.

On the other hand, within $SO(10)$ broken down to an intermediate $SU(3)_c \times SU(2)_L \times U(1)_R \times U(1)_{B-L}$ stage, only Z' and the associated $U(1)_R \times U(1)_{B-L} \to U(1)_Y$-breaking Higgs fields remain light (at least in minimally fine-tuned scenarios) and, thus, the intermediate-scale dynamics is generally much simpler than in the models based on the full $SU(2)_R \times U(1)_{B-L}$. In view of that, one can expect that also the intermediate-scale dependence of the soft RGE invariants will be much milder than in the former case. Moreover, with more than a single abelian gauge factor at play, there is a new class of effects associated with the so called kinetic mixing between the associated gauge fields. Both these aspects make this class of models worth further scrutiny.

1. General remarks

Remarkably, the simplicity of the minimally fine-tuned $U(1)_R \times U(1)_{B-L} \to U(1)_Y$ scenarios automatically implies the scale of this spontaneous symmetry breakdown is a sliding one. Indeed, minimal fine-tuning implies that the spectrum of the Model in the unbroken phase consists of that of the MSSM plus Z' plus an MSSM-neutral Higgs responsible for the relevant symmetry breaking. Since the gauge field associated to the hypercharge (B_Y) does not feel any effect of either Z' nor the hypercharge-neutral Higgs[6] the "effective" hypercharge gauge coupling (corresponding to a relevant combination of g_Y and g_R) in this picture runs as if it were in the MSSM, at least at the one-loop level. Thus, the specific position of the $U(1)_R \times U(1)_{B-L} \to U(1)_Y$ breaking scale is, in this case, irrelevant for the one-loop gauge running.

[6] To put this statement on a firm ground the effects of the kinetic mixing must be considered, see, e.g., [52].

Field	Mult.	$3_c 2_L 1_R 1_{B-L}$	$3_c 2_L 2_R 1_{B-L}$	$SO(10)$
Q	3	$(3,2,0,+\frac{1}{3})$	$(3,2,1,+\frac{1}{3})$	16
Q^c	3	$(\bar{3},1,\pm\frac{1}{2},-\frac{1}{3})$	$(\bar{3},1,2,-\frac{1}{3})$	16
L	3	$(1,2,0,-1)$	$(1,2,1,-1)$	16
L^c	3	$(1,1,\pm\frac{1}{2},+1)$	$(1,1,2,+1)$	16
S	3	$(1,1,0,0)$	$(1,1,1,0)$	1
Φ	2	$(1,2,\pm\frac{1}{2},0)$	$(1,2,2,0)$	10
Ω	1	absent	$(1,1,3,0)$	45
χ, $\overline{\chi}$	1	absent	$(1,2,1,\pm1)$	$\overline{16}$, 16
χ^c, $\overline{\chi}^c$	1	$(1,1,\pm\frac{1}{2},\mp1)$	$(1,1,2,\mp1)$	$\overline{16}$, 16

TABLE IV: The effective field contents of Model IV relevant to the two intermediate symmetry stages.

This, however, is not the case for the leading-log soft RGE invariants of our interest. In particular, unlike B_Y, both the $U(1)_R \times U(1)_{B-L}$ gauge bosons enter the renormalized propagators of squarks and sleptons

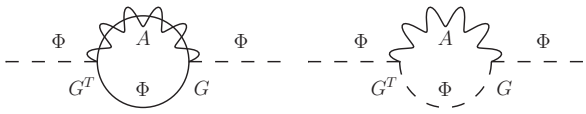

(2)

and one can expect a residual dependence of the invariants on the $U(1)_R \times U(1)_{B-L}$-breaking scale. Nevertheless, as we shall demonstrate in a particular realization of this simple scheme, such effects should be much milder than those in the scenarios with the full gauged $SU(2)_R$ symmetry.

2. Model IV: $U(1)_R \times U(1)_{B-L} \to U(1)_Y$ breaking

Here we consider a variant of the basic SUSY $SO(10)$ model advocated in [40] in which an extended intermediate $U(1)_R \times U(1)_{B-L}$ stage follows a short $SU(2)_R \times U(1)_{B-L}$ phase. The field content relevant to the RG running in the first two parts of the symmetry-breaking chain is given in TABLE IV.

In more detail, after the initial $SO(10) \to SU(3)_c \times SU(2)_L \times SU(2)_R \times U(1)_{B-L}$ breaking triggered by essentially the same mechanism as in Models I and II, the subsequent $SU(2)_R \times U(1)_{B-L} \to U(1)_R \times U(1)_{B-L}$ requires a VEV of the Ω field which, at the level of an effective theory, can again emerge from its interplay with a LR singlet. The last symmetry-breaking step is then

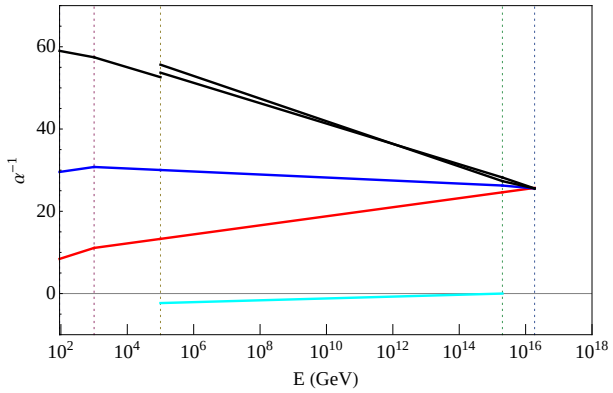

FIG. 4: Running in Model IV with a low $B-L$ scale. Note the effects of the U(1) mixing in the running & matching; the lowest curve corresponds to the off-diagonals of the $(GG^T/4\pi)^{-1}$ matrix.

achieved in a similar manner by the VEVs of the MSSM-neutral components of the $\chi^c \oplus \overline{\chi}^c$ fields.

The relevant b_i-coefficients at the $SU(3)_c \times SU(2)_L \times SU(2)_R \times U(1)_{B-L}$ level read $b_3 = -3$, $b_L = 2$, $b_R = 5$ and $b^{\rm can}_{B-L} = 15/2$. In the $SU(3)_c \times SU(2)_L \times U(1)_R \times U(1)_{B-L}$ stage, however, the effects of the $U(1)$ mixing must be taken into account and, thus, the b-coefficients in the $U(1)_R \times U(1)_{B-L}$ sector constitute a matrix of anomalous dimensions γ. One has $b_3 = -3$, $b_L = 1$ and

$$\gamma^{\rm phys} = \begin{pmatrix} 15/2 & -1 \\ -1 & 18 \end{pmatrix}, \qquad (3)$$

which should be brought into the canonical basis by means of a normalization matrix $N = {\rm diag}(1, \sqrt{3/8})$, $\gamma^{\rm can} = N\gamma^{\rm phys}N$. The details of the one-loop RGE evolution of gauge couplings and soft masses in theories with more than a single abelian gauge factor are summarized in Appendix A. The qualitative features of the gauge-coupling running in this setting can be seen in FIG. 4.

Concerning the flavour structure of the model, the situation is essentially identical to that described in the original work [40]. The only exception is a second LR bi-doublet retained until the $U(1)_R \times U(1)_{B-L}$ breaking scale which might be necessary in order to get a potentially realistic pattern of the effective Yukawa couplings. Nevertheless, the salient features of the Model in the soft sector should not depend much on the detailed realization of the effective Yukawa pattern.

III. LEADING-LOG RGE INVARIANTS

In this section we focus on the calculation of the invariants using mSugra boundary conditions. mSugra is defined at the GUT-scale, $M_{\rm G}$, by a common gaugino mass $M_{1/2}$, a common scalar mass m_0 and the trilinear coupling A_0, which gets multiplied by the corresponding Yukawa couplings to obtain the trilinear couplings in the soft SUSY breaking Lagrangian [7]. In addition, at the electro-weak scale, $\tan\beta = v_u/v_d$ is fixed. Here, as usual, v_d and v_u are the vacuum expectation values (vevs) of the neutral components of H_d and H_u, respectively. Finally, the sign of the μ parameter has to be chosen.

Renormalization group equations for general supersymmetric models are known up to 2-loop order [51]. The only case not covered in the otherwise general equations given in [51] are supersymmetric models with more than one $U(1)$ group. With more than a single abelian gauge factor, there appears a new class of effects associated with the so called kinetic mixing between the associated gauge fields. RGEs for this case have been derived very recently in [52].

Barring for the moment the effects of $U(1)$ mixing present in Model IV, at the 1-loop level, one can devise a simple set of analytic equations for the soft terms. Gaugino masses scale as gauge couplings do and so the requirement of GCU fixes the gaugino masses at the low scale

$$M_i(m_{SUSY}) = \frac{\alpha_i(m_{SUSY})}{\alpha(M_G)} M_{1/2}. \qquad (4)$$

Eq. (4) implies that the relationship of the M_i to $M_{1/2}$ is changed in Models I to III, since $\alpha(M_G)$ is shifted.

Neglecting the Yukawa couplings for the soft mass parameters of the first two generations of sfermions one can write

$$m^2_{\tilde f} \;=\; m_0^2 + \frac{M_{1/2}}{\alpha(M_{\rm G})^2} \sum_{R_j} \sum_{i=1}^{N} \tilde f_i^R \alpha_i(v_{R_j})^2 \,. \qquad (5)$$

Here, the sum over "R_j" runs over the different regimes in the models under consideration, while the sum over i runs over all gauge groups in a given regime. $\alpha_i(v_{R_j})$ is to

[7] It is sometimes argued that this setup should better be called CMSSM, since there are even simpler models of supergravity type breaking in which A_0 is not a free parameter, as for example in Polonyi type supergravity [53, 54]. Since we will be concerned with only the first two sfermion generations this distinction is irrelevant for us.

be understood as the gauge coupling of group i evaluated at the upper end of regime R_j. In the MSSM one would have only to consider one regime, namely from the SUSY scale to the GUT scale. In Models I and II we have two different regimes, while in Models III and IV there are a total of three regimes to consider.

The different $\tilde{f}_i^R$ can be written in a compact form as:

$$\tilde{f}_i^R \;=\; \frac{c_i^{f,R}}{b_i}\left[1-\left(\frac{\alpha_i(v_x)}{\alpha_i(v_y)}\right)^2\right], \tag{6}$$

where v_x and v_y, respectively, indicate the value of the relevant α at the lower and higher boundaries of the regime under consideration. The $c_i^{f,R}$ coefficients given in TABLE V are proportional to the values of the quadratic Casimir of representation R_f hosting the matter field f with respect to the group G in the regime R

$$c_i^{f,R} = 2C_G(R_f)\,. \tag{7}$$

They are readily evaluated from the basic formula

$$C_G(R)d(R) = T_2(R)d(G)\,, \tag{8}$$

where $d(G)$ is the dimension of the group G, $T_2(R)$ the Dynkin index of the representation R and $d(R)$ is its dimension. Note that the coefficients $c_i^{f,R}$ are different for the different fermions, which leads to a different coefficient in front of $M_{1/2}$ in eq. (5). The b_i in eq. (6) are the one-loop b-coefficients for the different models defined in the previous section. For completeness, the well-known one-loop beta-coefficients for the MSSM are (in the traditional $SU(5)$ normalization): $b = (b_1, b_2, b_3)^{MSSM} = (\frac{33}{5}, 1, -3)$.

Eq. (5) is valid neglecting $U(1)$-mixing effects. The extra effects due to the kinetic $U(1)$ mixing relevant in Model IV are summarized in the Appendix A; for a more detailed discussion including higher-loop effects, see [52].

Individual SUSY masses depend strongly on the initial values for m_0 and $M_{1/2}$. However, one can form four different combinations, which we choose to be

$$\begin{aligned} LE &\equiv (m^2_{\tilde{L}} - m^2_{\tilde{E}})/M_1^2, \\ QE &\equiv (m^2_{\tilde{Q}} - m^2_{\tilde{E}})/M_1^2, \\ DL &\equiv (m^2_{\tilde{D}} - m^2_{\tilde{L}})/M_1^2, \\ QU &\equiv (m^2_{\tilde{Q}} - m^2_{\tilde{U}})/M_1^2. \end{aligned} \tag{9}$$

It is easy to see that, at the leading-log level, m_0 and $M_{1/2}$ drop out of the equations for the invariants. Note, that one could have equally well normalized to any of the other two gaugino masses. The choice of M_1 is only motivated by the expectation that it will be the gaugino parameter measured with the smallest error.

$\tilde{f}$	$\tilde{E}$	$\tilde{L}$	$\tilde{D}$	$\tilde{U}$	$\tilde{Q}$
MSSM					
$c_1^{f,MSSM}$	$\frac{6}{5}$	$\frac{3}{10}$	$\frac{2}{15}$	$\frac{8}{15}$	$\frac{1}{30}$
$c_2^{f,MSSM}$	0	$\frac{3}{2}$	0	0	$\frac{3}{2}$
$c_3^{f,MSSM}$	0	0	$\frac{8}{3}$	$\frac{8}{3}$	$\frac{8}{3}$
$U(1)_R \times U(1)_{B-L}$					
$c_{BL}^{f,BL}$	$\frac{3}{4}$	$\frac{3}{4}$	$\frac{1}{12}$	$\frac{1}{12}$	$\frac{1}{12}$
$c_L^{f,BL}$	0	$\frac{3}{2}$	0	0	$\frac{3}{2}$
$c_R^{f,BL}$	$\frac{1}{2}$	0	$\frac{1}{2}$	$\frac{1}{2}$	0
$c_3^{f,BL}$	0	0	$\frac{8}{3}$	$\frac{8}{3}$	$\frac{8}{3}$
LR					
$c_{BL}^{f,LR}$	$\frac{3}{4}$	$\frac{3}{4}$	$\frac{1}{12}$	$\frac{1}{12}$	$\frac{1}{12}$
$c_L^{f,LR}$	0	$\frac{3}{2}$	0	0	$\frac{3}{2}$
$c_R^{f,LR}$	$\frac{3}{2}$	0	$\frac{3}{2}$	$\frac{3}{2}$	0
$c_3^{f,LR}$	0	0	$\frac{8}{3}$	$\frac{8}{3}$	$\frac{8}{3}$
Pati-Salam					
$c_L^{f,PS}$	0	$\frac{3}{2}$	0	0	$\frac{3}{2}$
$c_R^{f,PS}$	$\frac{3}{2}$	0	$\frac{3}{2}$	$\frac{3}{2}$	0
$c_4^{f,PS}$	$\frac{15}{4}$	$\frac{15}{4}$	$\frac{15}{4}$	$\frac{15}{4}$	$\frac{15}{4}$

TABLE V: Coefficients $c_i^{\tilde{f}}$ for eq. (5) for different symmetry stages. The MSSM and the LR parts are relevant to all four models under consideration; the $U(1)_R \times U(1)_{B-L}$ and the Pati-Salam parts are used solely for Model IV and Model III, respectively.

IV. SLIDING SCALE IMPRINTS IN THE LEADING-LOG RGE INVARIANTS

A. Models I and II with a sliding $SU(2)_R$ scale

The method: As we have already mentioned in Sect. II, in Models I and II the sliding nature of the $SU(2)_R$ scale makes it impossible to get an exact unification, in full analogy with the MSSM. Since, however, this is just about a 2% effect, we shall not attempt to improve on this by either looking for a suitable set of threshold corrections or by going beyond the one-loop approximation[8]. Rather than that, we shall just parametrize our ignorance of the "true values" of the unification scale position and the unified gauge coupling in terms of a pair of small "offset" parameters scanning over the area of the relevant "non-unification triangle" shown in FIG.(5). In what follows, we shall to use the error on $\alpha_S(M_Z)$ given

[8] Indeed, this would be inconsistent as we are concerned only with the leading-log approximation for the softs.

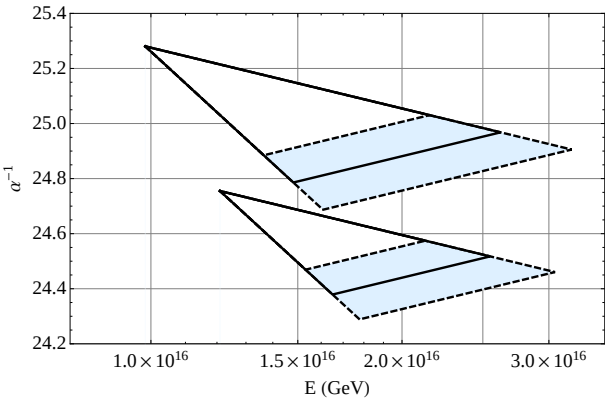

FIG. 5: The MSSM-like non-unification triangle in Models I and III with $v_R = 10^{14}$ GeV for two different values of the unknown soft-SUSY breaking scale ($m_{\rm SUSY} = 1$ TeV for the upper one and $m_{\rm SUSY} = 500$ GeV for the lower). The upper sides of the triangles corresponds to α_L^{-1} while the lower-left sides depict the "effective" α_Y^{-1} defined as $\frac{3}{5}\alpha_R^{-1} + \frac{2}{5}\alpha_{B-L}^{-1}$. The light blue area surrounding the α_S^{-1} line represents the 1σ uncertainty in $\alpha_s(M_Z)$ as given in [57]. Both triangles move down for lower values of v_R, see FIGs. 1 and 2.

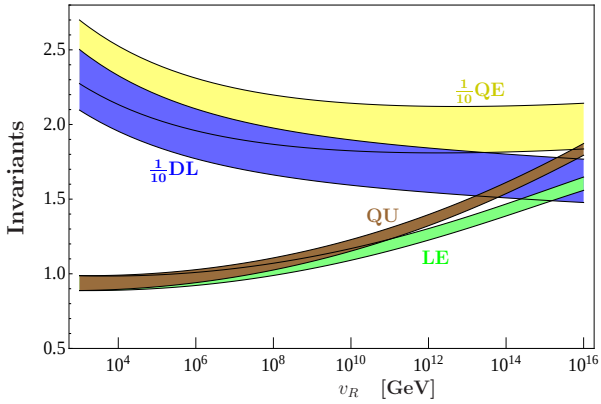

FIG. 6: The v_R-dependence of the leading-log invariants in Model I, c.f., Sect. II B 1 a. The bands represent the error due to the non-exact gauge-coupling unification depicted in FIG.5. For practical reasons, the numerical values of the invariants QE and DL have been scaled down by a factor of ten.

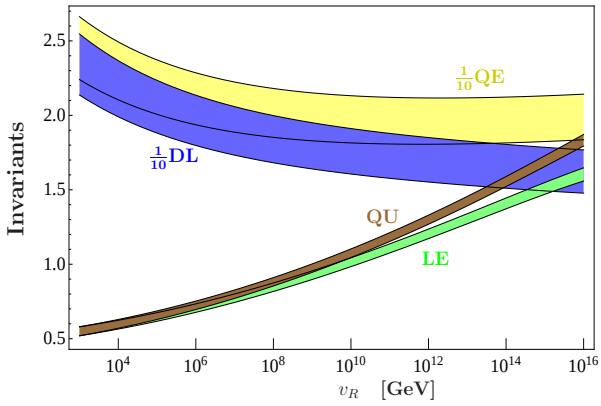

FIG. 7: The same as in FIG. 6 but for Model II of Sect. II B 1 b. The QU and LE behaviour differs from that in FIG. 6 mainly in the low-v_R regime.

in [57], $\Delta(\alpha_S(M_Z)) = 0.002$, which does not take into account the latest QCD lattice calculations results.

The results: In FIGs. 6 and 7 we display the v_R-dependence of the RGE invariants in Models I and II due to the running effects subsumed by Eq. (5). The bands correspond to the error in the gauge-coupling unification inherent to these settings which, at the leading-log level, can be taken into account by scanning over the area of the relevant non-unification triangle, c.f., FIG. 5. The upper (yellow) band refers to the combination QE, the (blue) band which at low v_R partially overlaps with QE represents DL, whereas the third (brown) band is QU and, finally, the lowest (green) band refers to the LE combination. Note that, for practical reasons, the invariants QE and DL have been scaled down by a factor of ten. The same colour-code is adopted in the other figures in this section.

Several comments are in order here: In general, the invariants exhibit a logarithmic dependence on v_R. For v_R close to the MSSM scale (on the left), the QU and LE invariants overlap. This is attributed to the enhanced gauge symmetry throughout the whole $m_{\rm SUSY}$-$M_{\rm G}$ range which makes $m^2_{\tilde{Q}}$ and $m^2_{\tilde{U}}$ as well as $m^2_{\tilde{L}}$ and $m^2_{\tilde{E}}$ behave the same, see the LR-stage $c_i^{\tilde{f}}$-coefficients in TABLE V. In the $v_R \to M_{\rm G}$ limit, the mSugra values of the invariants (modulo the MSSM non-unification) are reproduced. Concerning QE and DL, the first thing to notice is that these invariants tend to increase with v_R departing from $M_{\rm G}$, thus leading to a pattern characteristic to this class of models. Moreover, they are more sensitive to the initial condition because the colour-effects in their evolution do not cancel, thus leading to larger bands.

Naturally, the main difference between FIG. 7 and FIG. 6 is expected in the low-v_R regime where the effects due to the slight difference in the Model-I and Model-II spectra are most pronounced and the QU and LE invariants run faster due to a larger ratio of the coupling constants in the relevant Eq. (6).

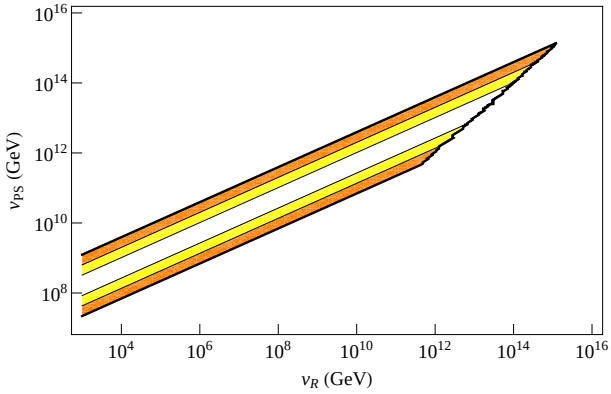

FIG. 8: The correlation of the intermediate symmetry-breaking scales in Model III (allowed region coloured). The contours correspond to the quality of the fit of $\alpha_S(M_Z)$ for each choice of the Pati-Salam breaking scale v_{PS} an the LR breaking scale v_R, within 1σ (white area within the coloured band), 2σ (yellow) and 3σ (orange) of the range quoted in [57].

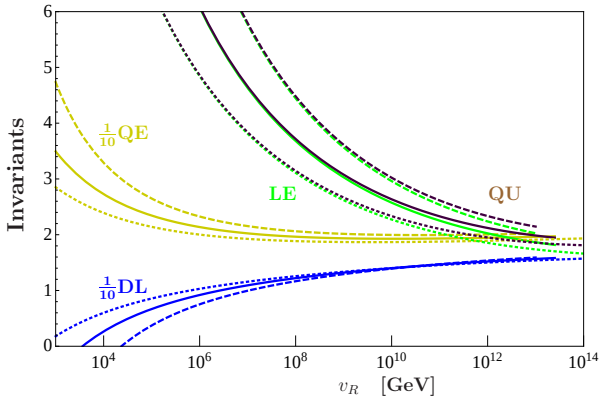

FIG. 9: Intermediate-scale dependence of the RGE invariants Model III, see Sect. II B 2. For each of the four invariants, the solid curve corresponds to $\alpha_S(M_Z)$ fixed at its central value and the dashed and dotted lines refer to the -1σ and $+1\sigma$ trajectories, respectively; c.f. FIG 8.

B. Model III with sliding $SU(2)_R$ and PS scales

The method: In Model III, the LR and PS intermediate scales can be always adjusted so that one gets an exact one-loop unification for v_R stretching up to about 10^{14} GeV, c.f., FIG. 8. This is technically achieved by relating the value of the PS scale to the value of the LR scale as

$$t_{PS} = \frac{1}{2}t_{LR} - \frac{1}{12}\Big(14t_{SUSY} + 20t_Z + \pi(18\alpha_S(t_Z)^{-1} - 33\alpha_L(t_Z)^{-1} + 15\alpha_Y(t_Z)^{-1})\Big) \quad (10)$$

Here, the t_x stand for $ln(m_X)$ as usual. Thus, the main uncertainty at this level comes from the experimental error in $\alpha_S(M_Z)$. In what follows, we shall vary v_R and v_{PS} along the constant $\alpha_S(M_Z)$-error trajectories, namely, within $\pm1\sigma$, corresponding to the boundaries between the yellow and white areas within the parameter area depicted in FIG. 8.

The results: In this case, the intermediate-scale dependence of the leading-log RGE invariants is yet more pronounced than in Models I and II, c.f., FIG 9. As before, the numerical values of the invariants QE and DL have been conveniently scaled down by a factor of ten. For each of the four invariants, the colid curve FIG 9 corresponds to $\alpha_S(M_Z)$ fixed at its central value and the dashed and dotted lines refer to the -1σ and $+1\sigma$ trajectories, respectively. On the high-v_R tail, the different curves stop at different energies due to the need to respect the natural $v_R < v_{PS}$ hierarchy reflected by the "diagonal" cut to the parametric space in FIG. 8.

For all four invariants under consideration, we observe a stronger v_R-dependence than in Models I and II. This is namely due to the extended Pati-Salam running which contributes with larger $c_i^{\tilde{f}}$-coefficients than the LR stage, c.f., TABLE V. Moreover, unlike in FIGs. 6 and 7, three out of four invariants grow with lowering v_R while the fourth one even becomes negative for v_R close to the MSSM scale, thus, again, leading to a very characteristic pattern.

C. Model IV with a sliding $U(1)_R \times U(1)_{B-L}$ scale

The method: Finally, in Model IV, c.f. Sect. II C, the unification is exact for any value of the sliding scale v_{BL} below a (constant) v_R in the ballpark of roughly 3×10^{15} GeV, c.f., FIG. 10. Thus, as before, the main uncertainty at this level comes from the experimental error in $\alpha_S(M_Z)$ which translates into small shifts in v_R. In what follows, we shall again vary v_{BL} along the constant $\alpha_S(M_Z)$-error trajectories, namely, within $\pm1\sigma$, corresponding to the boundaries between the yellow and white areas within the parametric depicted in FIG. 10.

The results: In the two panels of FIG. 11, the four invariants of our interest are depicted as functions of v_{BL}. As in the case of Model III, for each of them the solid line corresponds to the central-value trajectory in the parametric space of FIG. 10, whereas the dashed and dotted curves refer to the -1σ and $+1\sigma$-trajectories, respectively.

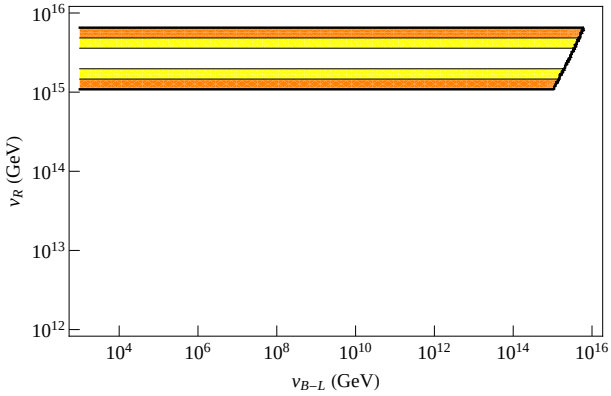

FIG. 10: The parameter space of Model IV of Sect. II C. The contours correspond to the different quality of the $\alpha_S(M_Z)$ fit for different choice of the L-R breaking scale v_R, namely, to 1σ (white), 2σ (yellow) and 3σ (orange) values for the range quoted in [57].

Due to the very special nature of the sliding scale in this setting, all four invariants exhibit only a very mild v_{BL} dependence, with the strongest effect of the order of few per cent observed in the LE case. This is because the v_{BL} scale enters into the soft masses only through the slight changes in the abelian gauge couplings, which, however, are overwhelmed by the colour effects in all the other invariants. This, however, will make it rather difficult to distinguish this model from the MSSM, namely because such a discrimination is efficient only if more than a single invariant differs significantly from the mSugra value so that the intermediate scale can be independently constrained from more than a single quantity.

Finally, let us comment in brief on the case where the $U(1)_R \times U(1)_{B-L} \to U(1)_Y$ breakdown is not triggered by $SU(2)_R$ doublets like above but by, e.g., $SU(2)_R$ triplets. We expect that for such models the effects on the invariants would be similar to those expected in Model IV, and certainly smaller than those observed in Models I-III.

D. Squark and slepton spectra.

In FIG. 12 we plot the shapes of the MSSM squark and slepton spectra obtained in mSugra and in Models I, II and III calculated for the SPS3 benchmark point, i.e. for $m_0 = 90$ GeV and $M_{1/2} = 400$ GeV. This figure is to be understood only as an illustrative example of the different spectra generated in our different models. For each of the cases, the horizontal lines (bottom to up) correspond to $m_{\tilde{e}^c}$ (light blue), $m_{\tilde{l}}$ (blue), $m_{\tilde{u}^c}$ (orange), $m_{\tilde{d}^c}$ (light orange) and $m_{\tilde{q}}$ (purple). In order to pronounce the differences, the v_R scale has been in all cases chosen very low, namely, $v_R \sim 10^3$ GeV, and consequently v_{PS} in Model III is fixed to $v_{PS} \sim 10^7$ GeV by gauge unification. The masses of the $\tilde{d}^c$ and of the $\tilde{u}^c$ almost coincide in all the Models. Models I and II differ from the mSugra case namely by the smaller splittings observable in the squark as well as in the slepton masses, which is more pronounced for the latter model. However, the spectrum of Model III is strongly compressed due to an extended Pati-Salam stage which makes it rather outstanding.

We decided not to overpopulate the figure by displaying the gaugino masses which, indeed, are obtained by a simple rescaling (4); the SUSY-to-GUT-scale ratios of the relevant α's can be inferred from the evolution of the gauge couplings, c.f. FIGs 1, FIGs 2, FIGs 3 and FIGs 4.

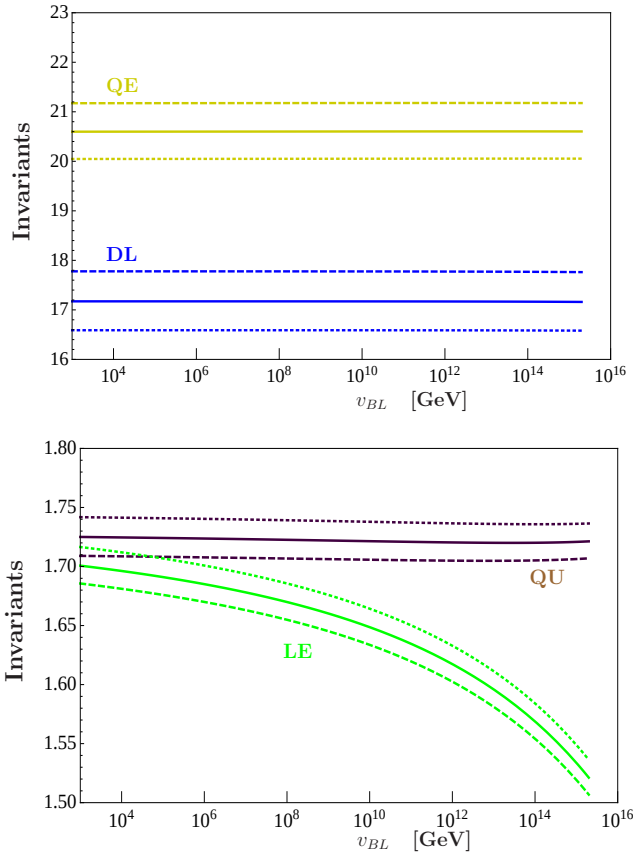

FIG. 11: The v_{BL}-scale dependence of the RGE invariants in Model IV. For practical purposes the figure has been split into two panels. For each of the four invariants, the colid curves correspond to $\alpha_S(M_Z)$ fixed at its central value while the dashed and dotted lines refer to the -1σ and $+1\sigma$ trajectories corresponding to roughly $v_R \sim 2\times10^{15}$ GeV and $v_R \sim 4\times10^{15}$ GeV, respectively; c.f. FIG 10.

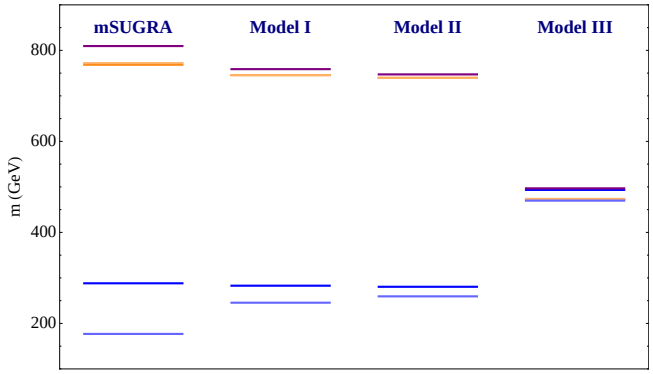

FIG. 12: The MSSM squark and slepton spectra mSugra and Models I, II and III calculated for the SPS3 benchmark point, i.e. for $m_0 = 90$ GeV and $M_{1/2} = 400$ GeV. In all cases, $v_R = 10^3$ GeV and $v_{PS} \sim 10^7$ GeV in Model III . From botton to up the horizontal lines correspond to: $m_{\tilde{e}^c}$ (light blue), $m_{\tilde{l}}$ (blue), $m_{\tilde{u}^c}$ (orange), $m_{\tilde{d}^c}$ (light orange) and $m_{\tilde{q}}$ (purple). We do not show the results for model IV in this figure, since they are very similar to the mSugra case.

V. DISCUSSION AND OUTLOOK

We have studied the leading-log RGE evolution of the MSSM soft SUSY breaking parameters for four different GUT models with mSugra boundary conditions. Although all the settings are based on the unified $SO(10)$ gauge group, they differ at the level of intermediate scale symmetry groups and/or particle content below the GUT scale. Two of the models discussed (Models I and II of Sects. II B 1 a and II B 1 b), which differ only in their beyond-MSSM field contents, feature an intermediate left-right symmetry which, at the level of precision used in this calculation, can be broken to $SU(3)_c \times SU(2)_L \times U(1)_Y$ of the MSSM almost anywhere between $M_{\rm G}$ and the soft SUSY-breaking scale. In Model III (c.f., Sect. II B 2) the sliding nature of the $SU(2)_R$-breaking scale relies on an additional intermediate Pati-Salam symmetry. Finally, in Model IV (see Sect. II C), the left-right symmetry is broken at a relatively high scale, but there is instead a sliding scale corresponding to the breaking of its $U(1)_R \times U(1)_{B-L}$ remnant. All models we consider are able to accommodate the neutrino data by either inverse or linear seesaw.

The extra gauge groups and/or beyond MSSM fields change the evolution of the soft parameters with respect to the basic mSugra expectation. The invariant mass combinations we considered are especially suited to uncover the effects of beyond-mSugra physics on the SUSY spectra. Remarkably, while invariants contain only a logarithmic dependence on the new physics scales, their behavior is *qualitatively* different in different models.

In our Models I and II, the invariants LE and QU (c.f., Sect. III) are always lower than the mSugra limit, while DL and QE are always larger. The former is a direct consequence of the LR symmetry, while the latter reflects mainly the shift in $\alpha(M_{\rm G})$ the models exhibit with respect to the MSSM expectation. Moreover, in spite of only a mild difference in the particle content, the invariants differ quantitatively between Model I and Model II.

In contrast to that, in the Pati-Salem based Model III, LE and QU are always larger than in mSugra, with a rather strong dependence on the v_R scale, namely due to the higher dimensionality of the relevant multiplets at the Pati-Salam stage. At the same time, in Model III, DL is always below the mSugra limit, while QE hardly varies at all as a function of v_R. Finally, Model IV is an example of how a new scale can be effectively "hidden" from the RGE invariants in special constructions: Despite containing a new scale potentially as low as $\mathcal{O}(1)$ TeV, all invariants are always very close to the mSugra limit in this model. Technically, this is achieved by maintaining the beta coefficients for the $SU(2)_L$ and $SU(3)_c$ factors as in the MSSM all the way up to a scale close to $M_{\rm G}$, while the sliding feature of the $U(1)_R \times U(1)_{B-L}$ breaking scale "shields" all invariants from the effects of the new group, with the exception of LE, which, however, changes only very weakly.

It is especially interesting to compare our results with those obtained for minimal seesaw models within mSugra. Invariants for seesaw have been studied previously in [28, 47, 49]. Type-I seesaw adds only singlets to the MSSM and thus, just like our Model IV, can not be distinguished from the pure mSugra case by means of the invariants only. Type-II and type-III seesaw, on the other hand, change the b-coefficients with respect to the MSSM, but do not extend the gauge group. As a result, for minimal seesaws all four invariants are larger than their mSugra limit if the seesaw scale is below the GUT scale, as indicated by neutrino data. Thus, the invariants should allow to distinguish our $SO(10)$-based Models I to III from type-II and type-III seesaw.

The RGE invariants are, therefore, good model discriminators, at least in principle. However, any attempt to quantitatively determine the scale of a new physics within a particular scenario must inevitably address the accuracy of their calculation. Different types of errors need to be considered here. First, there are the errors

from uncertainties in the values of the input parameters. The largest error currently stems from the completely unknown m_{SUSY}, see FIG. 5 and Eq. (4). Once SUSY masses, indeed, have been measured, this will become irrelevant and the largest error will, most likely, be $\Delta(\alpha_S)$.

Next, the RGE invariants considered here are calculated to the leading-log precision only. However, in some cases, important higher order effects such as genuine 2-loop corrections and 1-loop thresholds can emerge; for the seesaw, this was studied recently in [28, 49]. Both, 2-loop running and 1-loop SUSY thresholds can, of course, be taken into account, but the calculation of the invariants at this level can not be done analytically. Instead, it requires numerical tools such as, e.g., SPheno [58, 59] and SARAH [60–62].

Probably more important than the above theoretical considerations, eventually, will be the fact that the invariants are not directly measurable quantities. Conversion of the invariants into the measured sparticle masses (or extraction of relevant soft parameters from sparticle measurements) requires additional *experimental* input. In case of the first two generations of sfermions this requires at least a reliable measurement of $\tan\beta$ for the determination of the D-terms. In addition, at variance with the situation in the minimal seeesaw models, the breaking of the extra gauge symmetries can potentially produce new D-terms not present in the $SU(3)_C \times SU(2)_L \times U(1)_Y$ case. Usually it is assumed that any beyond-SM gauge group is broken in a "D-flat" manner in order to avoid problems with tachyonic sfermions. However, since we wish to extract information from sfermion masses themselves, it will certainly be prudent to do a combined fit on the new parameters instead of simply *assuming* D-flatness.

The prospects of measuring sparticle masses at the LHC and, possibly, at the future ILC have been studied by many authors, for a detailed review see, for example [6]. In general, one expects that slepton and gaugino masses, if within the kinematical reach of the ILC, can be measured at the per mill level or even better. Coloured sparticles, however, might be too heavy to be produced at the ILC. At the LHC, the precision with which sparticle masses can be measured depends strongly not only on the absolute scale of the SUSY masses, but also decisively on the mass ordering of the sparticles. If long decay chains such as $\tilde{q} \to \chi_2^0 q$ with $\chi_2^0 \to \tilde{l}l \to l^\pm l^\mp \chi_1^0$ are available, many SUSY masses can be measured with accuracies down to (few) percent. From the detailed studies of [6], the authors of [50] concluded that the precision of ILC+LHC combined would make it possible to see indications for a seesaw of either type II or type III for nearly all relevant seesaw scales. In an LHC-only analysis, the seesaw scale must be below 10^{14} GeV even in favourable circumstances [50] or might not leave a trace in the LHC data at all.

Comparing roughly the changes in spectra induced in the seesaw models studied in [50] with the changes expected in our $SO(10)$ models, we expect that a detailed, numerical calculation should be able to probe most, if not all the interesting parameter space of our models, if SUSY is found at the LHC and precise mass measurements are done with the help of an ILC.

Finally, we would like to mention that the models we have studied in this paper have potentially also a rich phenomenology beyond the MSSM apart from the invariants. There are the new gauge bosons, additional Higgses, additional gauginos/higgsinos, large lepton flavour violation and many other effects worth studying. We plan to return to these questions in a future publication.

Acknowledgments

The work of V D R is supported by the EU Network grant UNILHC PITN-GA-2009-237920. M. M. is supported by the Marie Curie Intra European Fellowship within the 7th European Community Framework Programme FP7-PEOPLE-2009-IEF, contract number PIEF-GA-2009-253119. We acknowledge support from the Spanish MICINN grants FPA2008-00319/FPA and MULTIDARK CAD2009-00064 (Con-solider-Ingenio 2010 Programme) and by the Generalitat Valenciana grant Prometeo/2009/091.

Appendix A: One-loop running with U(1) mixing

In this appendix we give some technical details of the one-loop evolution of gauge couplings and soft-SUSY-breaking terms in Model IV of Sect. II C in which extra kinetic mixing effects, generally present in theories with multiple $U(1)$ gauge factors, emerge. This, in the approach advocated in, e.g., [52], amounts to extending the notion of the individual gauge couplings and gaugino masses associated to different $U(1)$ gauge factors to matrix forms, which, subsequently, complicates the relevant generalized evolution equations.

a. Gauge couplings

To deal with the effects of the kinetic mixing in cases with more than a single abelian gauge factor like in Model IV of Sect. II C it is convenient to work with a matrix of gauge couplings rather than with each of them individually, which would require an extra RGE for the kinetic mixing parameters, c.f., [52]. In the $U(1)_R \times U(1)_{B-L}$ case this amounts to defining

$$G = \begin{pmatrix} g_{RR} & g_{RX} \\ g_{XR} & g_{XX} \end{pmatrix} . \tag{A1}$$

where X is a shorthand notation for the canonically normalized $B-L$. The evolution equation can be then written as

$$\frac{\mathrm{d}}{\mathrm{d}t} A^{-1} = -\gamma \,, \tag{A2}$$

where $A^{-1} \equiv 4\pi (GG^T)^{-1}$ and $t = \frac{1}{2\pi}\log(\mu/\mu_0)$. Here we have defined the relevant matrix of anomalous dimensions by

$$\gamma \equiv \sum_f Q_f Q_f^T \,, \tag{A3}$$

where the summation is taken over all the chiral superfields f in the model and Q_f denotes a column vector of $U(1)_R$ and $U(1)_{B-L}$ charges of each f.

The matching condition between such high-energy gauge couplings (corresponding to $U(1)_R \otimes U(1)_{B-L}$ in the case of our interest) and the effective-theory one (i.e., $U(1)_Y$ of the MSSM) at scale t_0 then reads

$$\alpha_Y^{-1}(t_0) = p_Y^T \, A^{-1}(t_0) p_Y \,, \tag{A4}$$

where $p_Y^T = (\sqrt{\frac{3}{5}}, \sqrt{\frac{2}{5}})$ are the coefficients of the hypercharge Y in the space of the R- and $B-L$-charges, namely, $Y = \sqrt{\frac{3}{5}} T_R^3 + \sqrt{\frac{2}{5}} X$. Thus, one has

$$\begin{aligned} g_Y^{-2} \;=\; & (g_{RR}g_{XX} - g_{RX}g_{XR})^{-2} \left[\frac{3}{5}\left(g_{XX}^2 + g_{XR}^2\right) \right. \\ & \left. + \frac{2}{5}\left(g_{RR}^2 + g_{RX}^2\right) - \frac{2}{5}\sqrt{6}\left(g_{RR}g_{XR} + g_{RX}g_{XX}\right) \right] . \end{aligned} \tag{A5}$$

b. Soft SUSY-breaking terms

Neglecting for simplicity the Yukawa couplings and also the "Trace-terms" (denoted by $\mathcal{S}$ in [51]), which in mSugra yield only sub-leading correction to the leading-log approximation used in this work, one can write the generalized evolution equation including the effects of the $U(1)$ mixing [52] as

$$\frac{\mathrm{d}}{\mathrm{d}t} \tilde{m}_f^2 = -\frac{1}{\pi} Q_f^T G M M^\dagger G^T Q_f \,, \tag{A6}$$

where G is the matrix of gauge couplings, M is the gaugino mass matrix and $t = \frac{1}{2\pi}\log\mu/\mu_0$. This is to be solved together with the gauge coupling (A2) and gaugino evolution equations. The latter reads at one loop

$$\frac{\mathrm{d}}{\mathrm{d}t} M = \frac{1}{8\pi}\left(MG^T\gamma G + G^T\gamma G M\right) . \tag{A7}$$

The simplicity of the system (A2), (A6) and (A7) and, in particular, the flavour-diagonal mSugra initial condition, admits to write the general solution in a closed and compact form

$$A^{-1}(t) \;=\; A^{-1}(t_0) - \gamma(t-t_0) \,, \tag{A8}$$

$$(G^{-1T} M G^{-1})(t) \;=\; \frac{1}{4\pi}\alpha_G^{-1} M_{1/2} \,, \tag{A9}$$

and, in particular,

$$\begin{aligned} \tilde{m}_f^2(t) - \tilde{m}_f^2(t_0) = 2M_{1/2}^2 \alpha_G^{-2} \times \\ Q_f^T A_0^{-1}\left[\gamma^{-1} - A^{-1}A_0\gamma^{-1}A_0A^{-1}\right] A_0^{-1} Q_f \,, \end{aligned} \tag{A10}$$

where $A_0 \equiv A(t_0)$ and $A \equiv A(t)$.

[1] A. H. Chamseddine, R. L. Arnowitt and P. Nath, Phys. Rev. Lett. **49** (1982) 970.

[2] H. P. Nilles, Phys. Rept. **110** (1984) 1.

[3] For a review on GMSB, see: G. F. Giudice and R. Rattazzi, Phys. Rept. **322** (1999) 419 [arXiv:hep-ph/9801271].

[4] S. P. Martin and P. Ramond, Phys. Rev. D **48**, 5365 (1993) [arXiv:hep-ph/9306314].

[5] J. A. Aguilar-Saavedra *et al.* [ECFA/DESY LC Physics Working Group], arXiv:hep-ph/0106315.

[6] G. Weiglein *et al.* [LHC/LC Study Group], Phys. Rept. **426** (2006) 47 [arXiv:hep-ph/0410364].

[7] J. A. Aguilar-Saavedra *et al.*, Eur. Phys. J. C **46**, 43 (2006) [arXiv:hep-ph/0511344].

[8] G. A. Blair, W. Porod and P. M. Zerwas, Phys. Rev. D **63** (2001) 017703 [arXiv:hep-ph/0007107].

[9] G. A. Blair, W. Porod and P. M. Zerwas, Eur. Phys. J. **C27**, 263 (2003), [hep-ph/0210058].

[10] P. Bechtle, K. Desch, W. Porod and P. Wienemann, Eur. Phys. J. C **46** (2006) 533 [arXiv:hep-ph/0511006].

[11] R. Lafaye, T. Plehn, M. Rauch and D. Zerwas, Eur. Phys. J. C **54** (2008) 617 [arXiv:0709.3985 [hep-ph]].

[12] C. Adam, J. L. Kneur, R. Lafaye, T. Plehn, M. Rauch and D. Zerwas, arXiv:1007.2190 [hep-ph].

[13] Y. Fukuda *et al.* [Super-Kamiokande Collaboration], Phys. Rev. Lett. **81**, 1562 (1998)

[14] SNO, Q. R. Ahmad *et al.*, Phys. Rev. Lett. **89**, 011301 (2002), [nucl-ex/0204008].

[15] KamLAND, K. Eguchi *et al.*, Phys. Rev. Lett. **90**, 021802 (2003), [hep-ex/0212021].

[16] N. Arkani-Hamed and S. Dimopoulos, JHEP **0506**, 073 (2005) [arXiv:hep-th/0405159].

[17] G. F. Giudice and A. Romanino, Nucl. Phys. B **699**, 65 (2004) [Erratum-ibid. B **706**, 65 (2005)] [arXiv:hep-ph/0406088].

[18] KamLAND Collaboration, arXiv:0801.4589 [hep-ex].

[19] For a recent review on the status of neutrino oscillation data, see: T. Schwetz, M. A. Tortola and J. W. F. Valle, New J. Phys. **10**, 113011 (2008) [arXiv:0808.2016 [hep-ph]]. Version 3 on the arXive is updated with data until Feb 2010

[20] T. Schwetz, M. Tortola and J. W. F. Valle, New J. Phys. **13**, 063004 (2011) [arXiv:1103.0734 [hep-ph]].

[21] E. Ma, Phys. Rev. Lett. **81**, 1171 (1998) [arXiv:hep-ph/9805219].

[22] P. Minkowski, Phys. Lett. B **67** (1977) 421.

[23] T. Yanagida, in *KEK lectures*, ed. O. Sawada and A. Sugamoto, KEK, 1979; M Gell-Mann, P Ramond, R. Slansky, in *Supergravity*, ed. P. van Niewenhuizen and D. Freedman (North Holland, 1979);

[24] R.N. Mohapatra and G. Senjanovic, *Phys. Rev. Lett.* **44** 912 (1980).

[25] J. Schechter and J. W. F. Valle, Phys. Rev. D **22**, 2227 (1980).

[26] T. P. Cheng and L. F. Li, Phys. Rev. D **22**, 2860 (1980).

[27] R. Foot, H. Lew, X. G. He and G. C. Joshi, Z. Phys. C **44**, 441 (1989).

[28] J. N. Esteves, J. C. Romao, M. Hirsch, F. Staub and W. Porod, Phys. Rev. D **83**, 013003 (2011) [arXiv:1010.6000 [hep-ph]].

[29] C. Biggio and L. Calibbi, arXiv:1007.3750 [hep-ph].

[30] H. Fritzsch and P. Minkowski, Annals Phys. **93** (1975) 193.

[31] R. N. Mohapatra and J. W. F. Valle, Phys. Rev. **D34**, 1642 (1986).

[32] E. Akhmedov, M. Lindner, E. Schnapka and J. W. F. Valle, Phys. Rev. **D53**, 2752 (1996), [hep-ph/9509255]; Phys. Lett. **B368**, 270 (1996), [hep-ph/9507275].

[33] R. N. Mohapatra, *Berlin, Germany: Springer (1986) 309 P. (Contemporary Physics)*

[34] M. Cvetic and J. C. Pati, Phys. Lett. B **135**, 57 (1984).

[35] R. Kuchimanchi and R. N. Mohapatra, Phys. Rev. D **48**, 4352 (1993) [arXiv:hep-ph/9306290].
[36]

[36] C. S. Aulakh, K. Benakli and G. Senjanovic, Phys. Rev. Lett. **79**, 2188 (1997) [arXiv:hep-ph/9703434].

[37] C. S. Aulakh, A. Melfo, A. Rasin and G. Senjanovic, Phys. Rev. D **58**, 115007 (1998) [arXiv:hep-ph/9712551].

[38] J. Kopp, M. Lindner, V. Niro and T. E. J. Underwood, Phys. Rev. D **81**, 025008 (2010) [arXiv:0909.2653 [hep-ph]].

[39] S. K. Majee, M. K. Parida, A. Raychaudhuri and U. Sarkar, Phys. Rev. D **75**, 075003 (2007) [arXiv:hep-ph/0701109].

[40] M. Malinsky, J. C. Romao and J. W. F. Valle, Phys. Rev. Lett. **95**, 161801 (2005) [arXiv:hep-ph/0506296].

[41] P. S. B. Dev and R. N. Mohapatra, Phys. Rev. D **81** (2010) 013001 [arXiv:0910.3924 [hep-ph]].

[42] K. Nakamura *et al.* [Particle Data Group], J. Phys. G **37**, 075021 (2010).

[43] G. Aad *et al.* [ATLAS Collaboration], Phys. Lett. **B700** (2011) 163-180. [arXiv:1103.6218 [hep-ex]].

[44] L. Basso, A. Belyaev, S. Moretti, G. M. Pruna and C. H. Shepherd-Themistocleous, Eur. Phys. J. C **71**, 1613 (2011) [arXiv:1002.3586 [hep-ph]].

[45] S. N. Gninenko, M. M. Kirsanov, N. V. Krasnikov and V. A. Matveev, Phys. Atom. Nucl. **70** (2007) 441.

[46] A. Ferrari *et al.*, Phys. Rev. D **62** (2000) 013001.

[47] M. R. Buckley and H. Murayama, Phys. Rev. Lett. **97**, 231801 (2006) [arXiv:hep-ph/0606088].

[48] J. C. Pati and A. Salam, Phys. Rev. D **10**, 275 (1974) [Erratum-ibid. D **11**, 703 (1975)].

[49] M. Hirsch, S. Kaneko and W. Porod, Phys. Rev. D **78**, 093004 (2008) [arXiv:0806.3361 [hep-ph]].

[50] M. Hirsch, L. Reichert and W. Porod, JHEP **1105**, 086 (2011) [arXiv:1101.2140 [hep-ph]].

[51] S. P. Martin and M. T. Vaughn, Phys. Rev. D **50**, 2282 (1994) [Erratum-ibid. D **78**, 039903 (2008)] [arXiv:hep-ph/9311340].

[52] R. Fonseca, M. Malinsky, W. Porod and F. Staub, arXiv:1107.2670 [hep-ph].

[53] J. R. Ellis, K. A. Olive, Y. Santoso and V. C. Spanos, Phys. Lett. B **573**, 162 (2003) [arXiv:hep-ph/0305212].

[54] S. P. Martin, arXiv:hep-ph/9709356.

[55] L. Lavoura, H. Kuhbock, and W. Grimus, Nucl.Phys. **B754**, 1 (2006), arXiv:hep-ph/0603259.

[56] M. Heinze and M. Malinsky, Phys.Rev. **D83**, 035018 (2011), arXiv:1008.4813.

[57] C. Amsler *et al.* [Particle Data Group], Phys. Lett. B **667**, 1 (2008).

[58] W. Porod, Comput. Phys. Commun. **153**, 275 (2003) [arXiv:hep-ph/0301101]. For the latetst version of SPheno, see the web page: http://www.physik.uni-wuerzburg.de/ porod/SPheno.html

[59] W. Porod and F. Staub, arXiv:1104.1573 [hep-ph].

[60] F. Staub, arXiv:0806.0538 [hep-ph].

[61] F. Staub, Comput. Phys. Commun. **181**, 1077 (2010) [arXiv:0909.2863 [hep-ph]].

[62] F. Staub, arXiv:1002.0840 [Unknown].